

Supplementary Information

Two-step synthesis of heterometallic coordination polymers using a polyazamacrocyclic linker

**J. Aríñez-Soriano, J. Albalad, J. Pérez-Carvajal, I. Imaz, F. Busqué, J. Juanhuix
and D. Maspoch**

Figure S1. Characterization of **1**: (a) ^1H -NMR (CDCl_3 , 298 K, 360 MHz), and (b) ^{13}C -NMR (CDCl_3 , 298 K, 90 MHz).

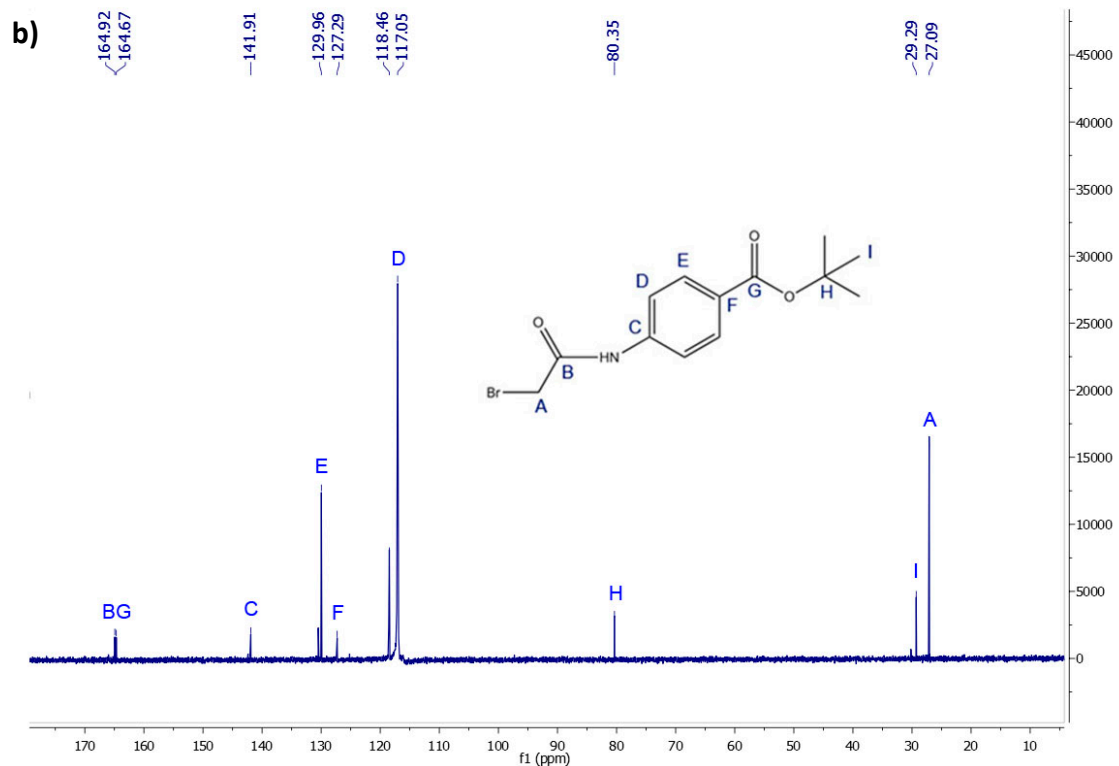
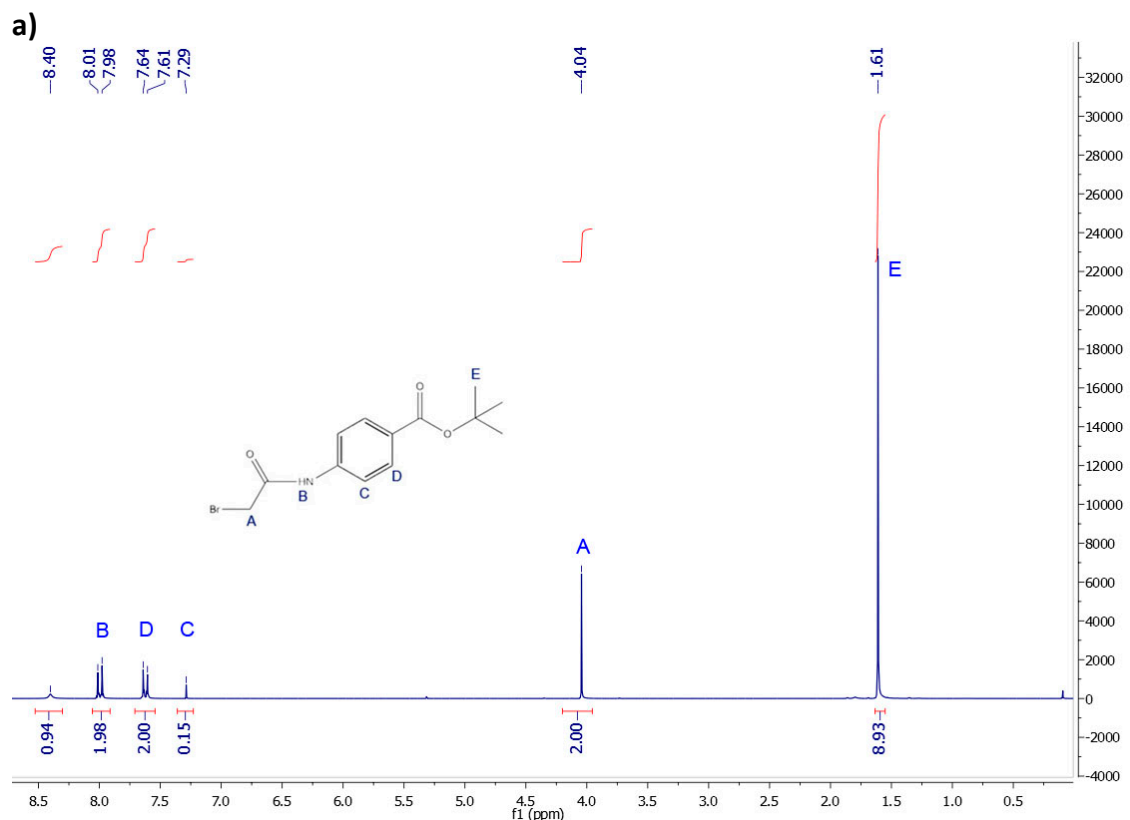
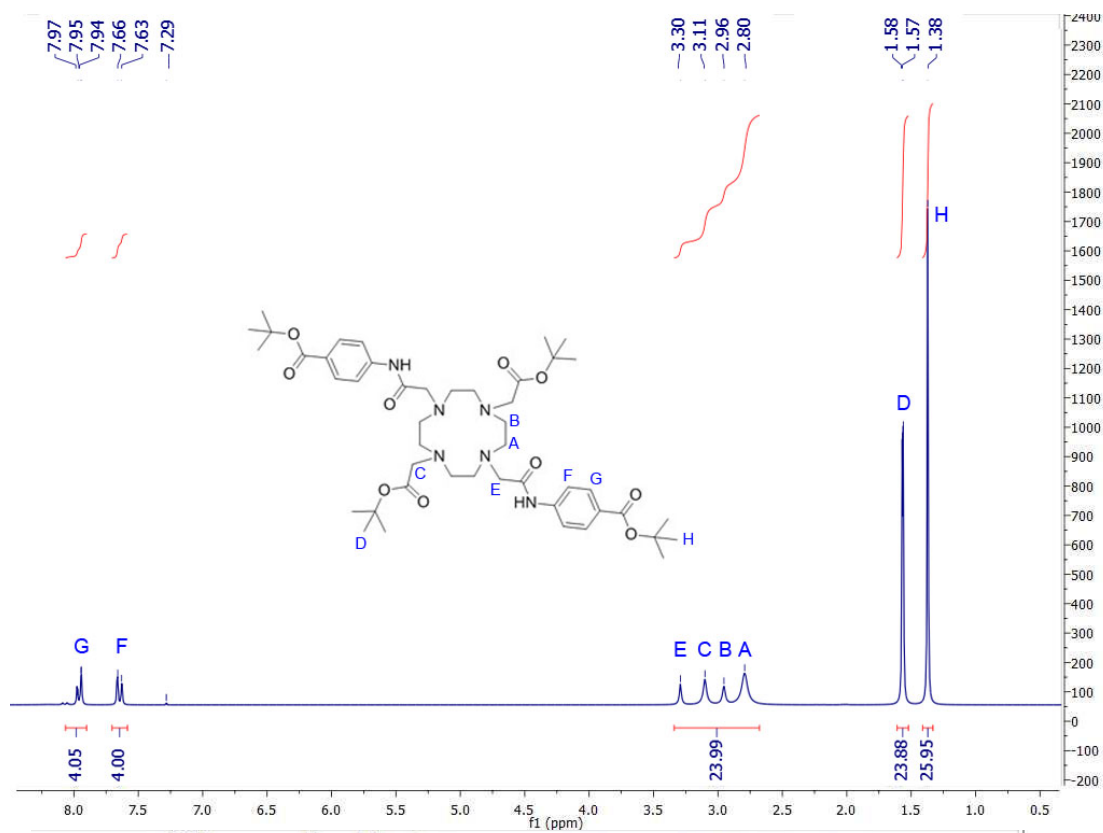
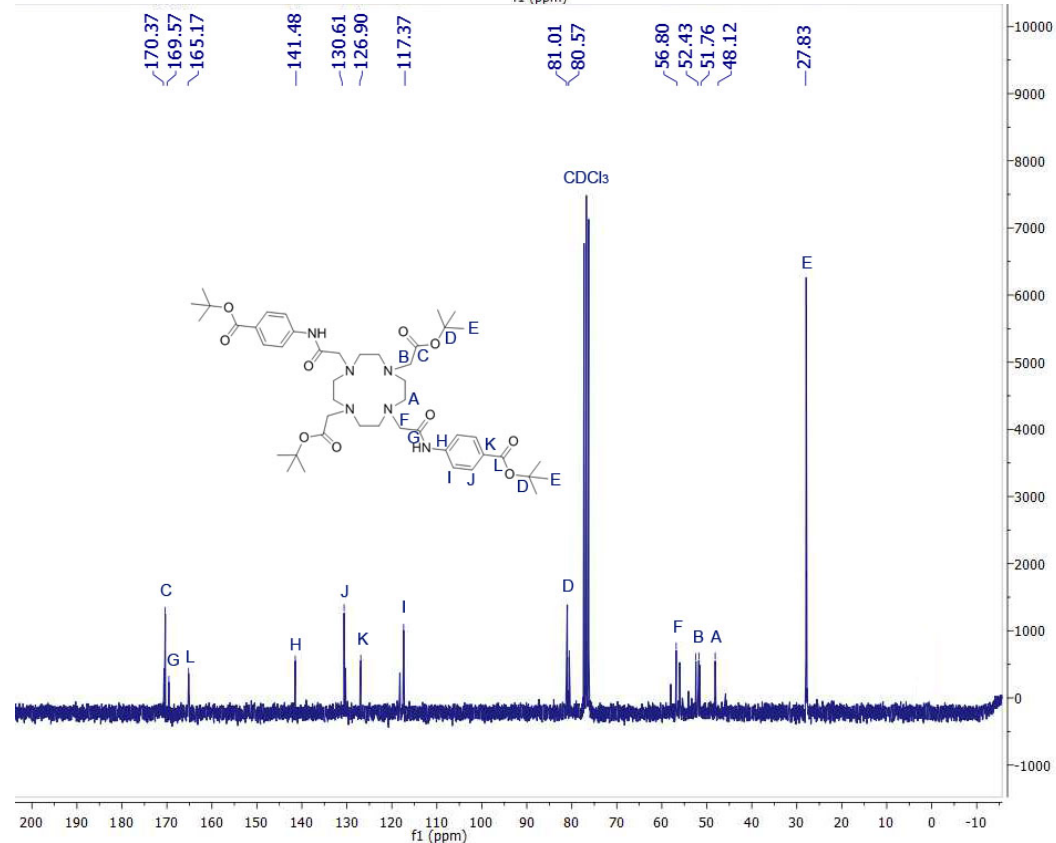


Figure S2. Characterization of **2**: (a) ^1H -NMR (CDCl_3 , 298 K, 360 MHz), (b) ^{13}C -NMR (CDCl_3 , 298 K, 90 MHz), and (c) ESI-TOF/MS spectrum.

a)



b)



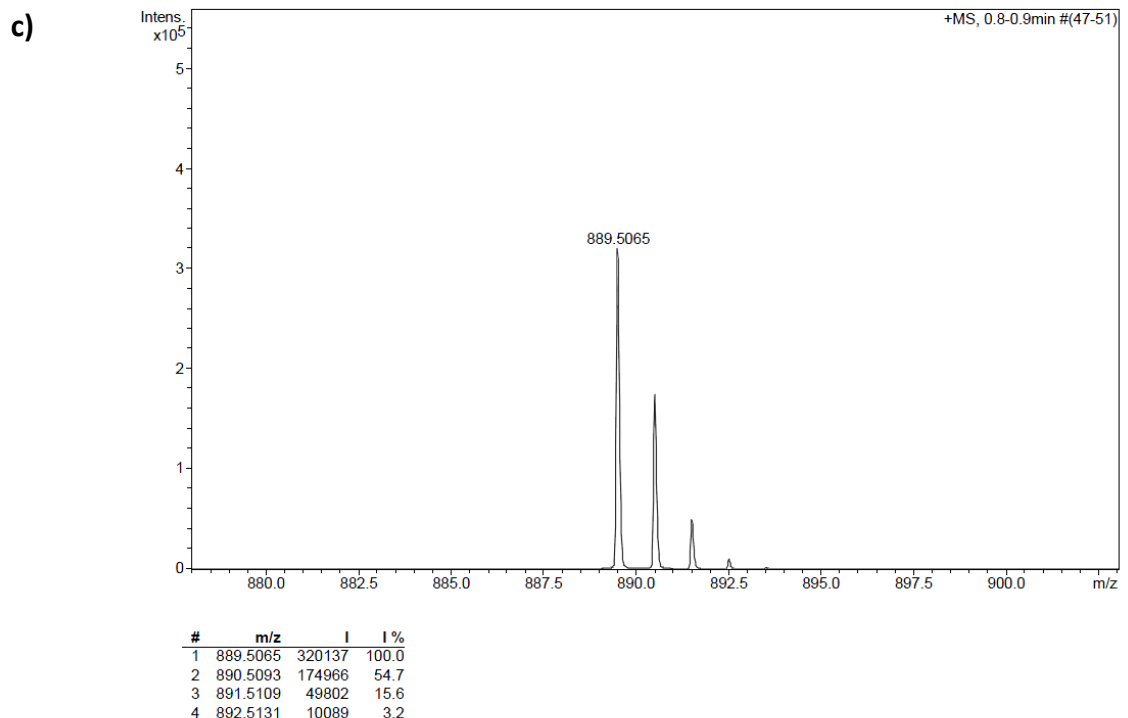
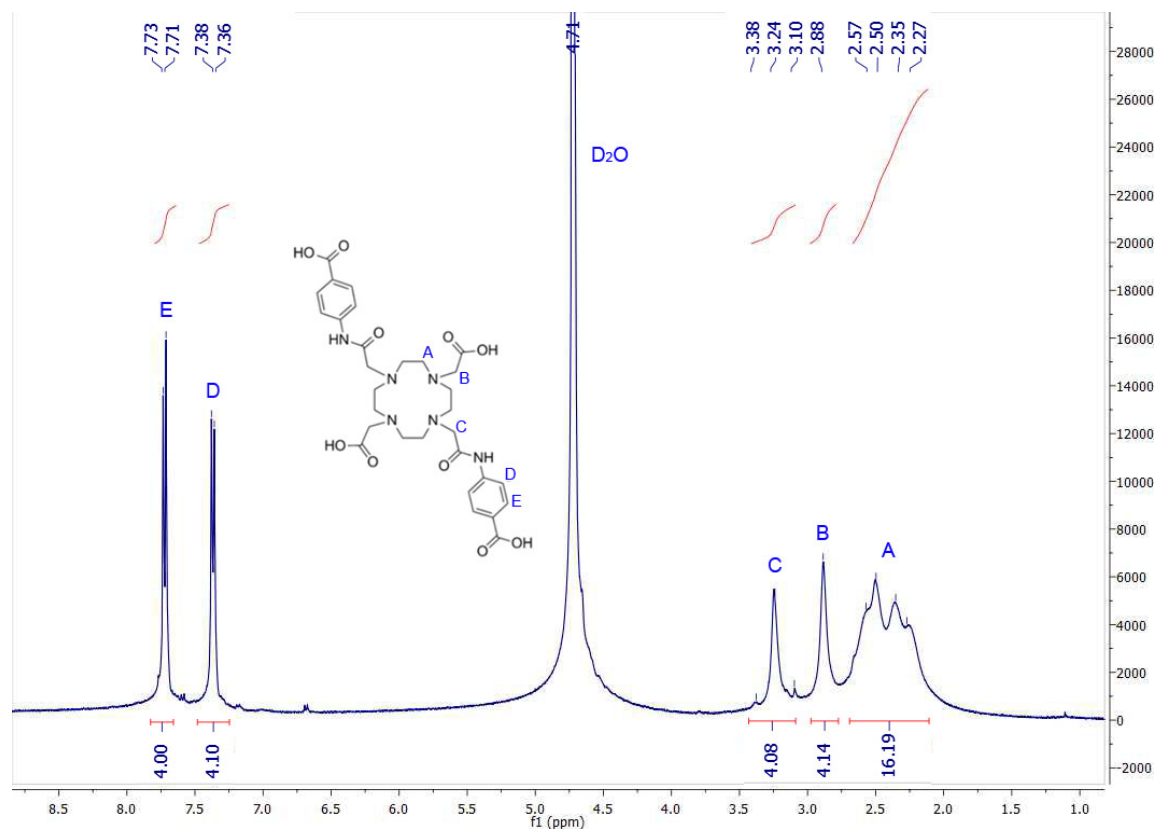
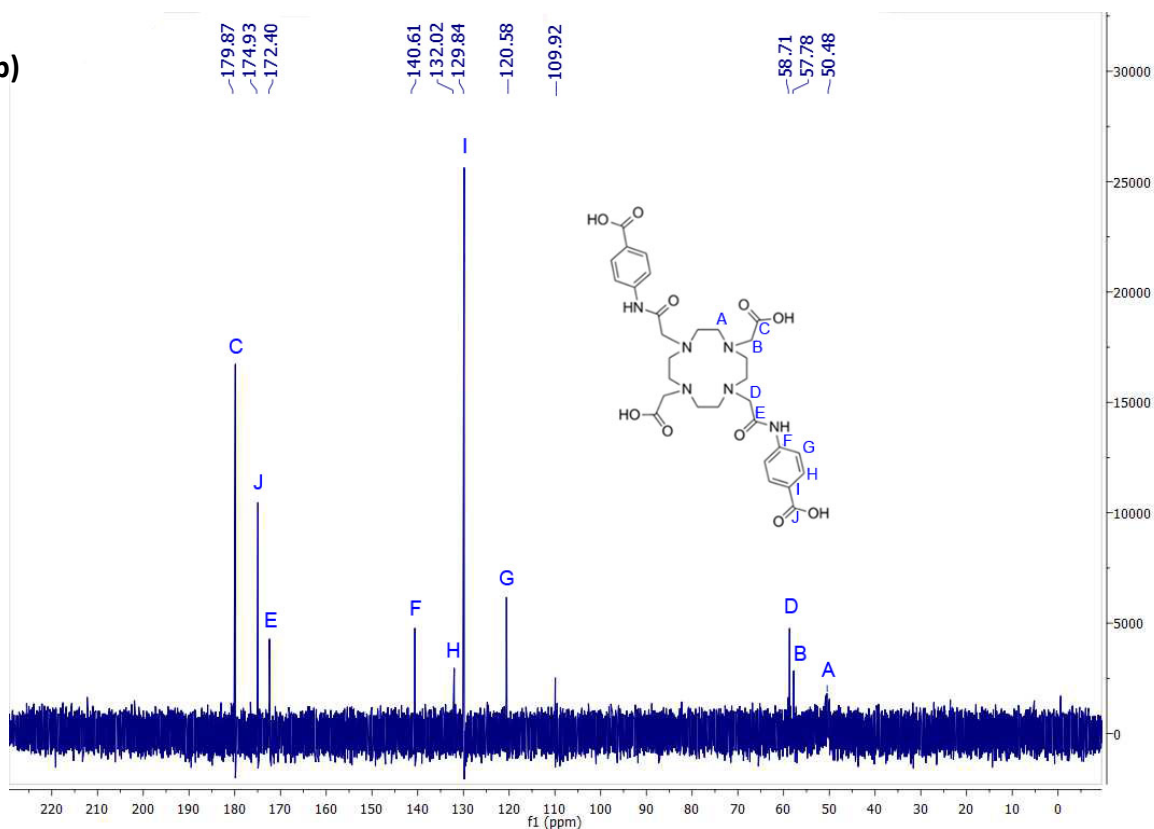


Figure S3. Characterization of H₄L1: (a) ¹H-NMR (D_2O , 298 K, 400 MHz), (b) ¹³C-NMR (D_2O , 298 K, 100 MHz), (c) ESI-TOF/MS spectrum, and (d) FT-IR spectrum.

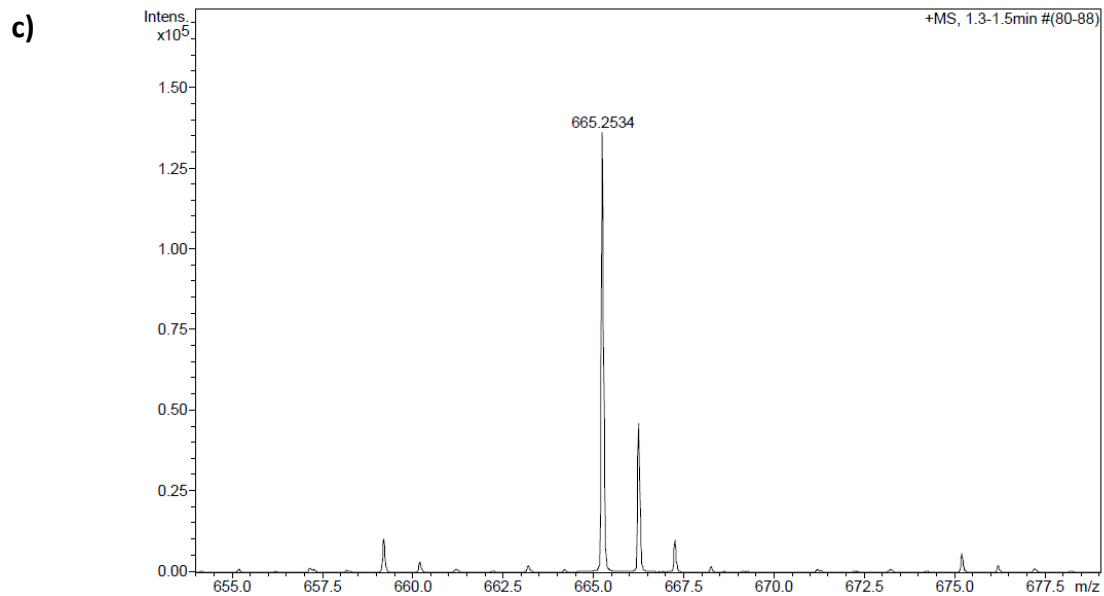
a)



H Label	δ (ppm)	Integration	Mult ($^3J_{\text{H-H}}$ (Hz))	Assignation
H _A	2.43	16H	mult	NCH ₂ CH ₂ N
H _B	2.88	4H	s	NCH ₂ CONH
H _C	3.38	4H	s	NCH ₂ COO
H _D	7.37	4H	d (7.5 Hz)	Ar
H _E	7.72	4H	d (7.5 Hz)	Ar

b)

C Label	δ (ppm)	Assigmentation
C _A	50.5	NCH ₂ CH ₂ N
C _B	55.8	NCH ₂ COO
C _C	179.9	CH ₂ COO
C _D	58.7	NCH ₂ CONH
C _E	172.3	Ar-COO
C _F	140.6	NH-Ar
C _G	120.6	Ar
C _H	132.0	Ar
C _I	129.8	Ar-COO
C _J	174.9	CH ₂ CONH



#	m/z	I	I %
1	665.2534	136128	100.0
2	666.2559	46190	33.9
3	667.2580	10070	7.4
4	668.2586	1706	1.3

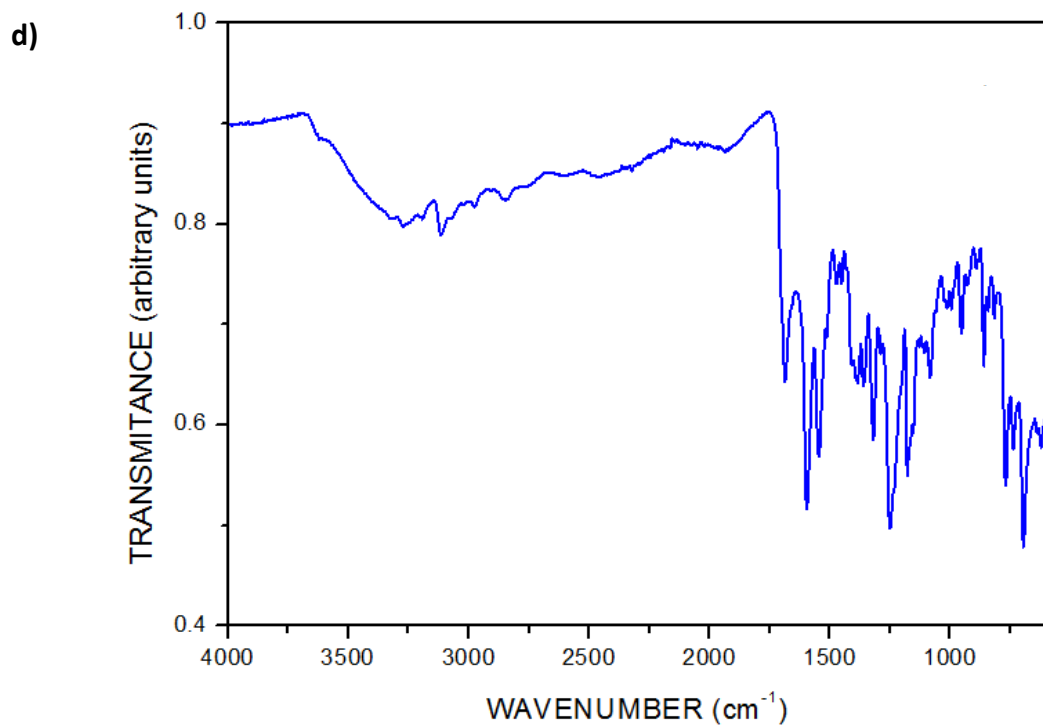


Figure S4. Characterization of **3**: (a) ESI-TOF/MS spectrum, and (b) FT-IR spectrum.

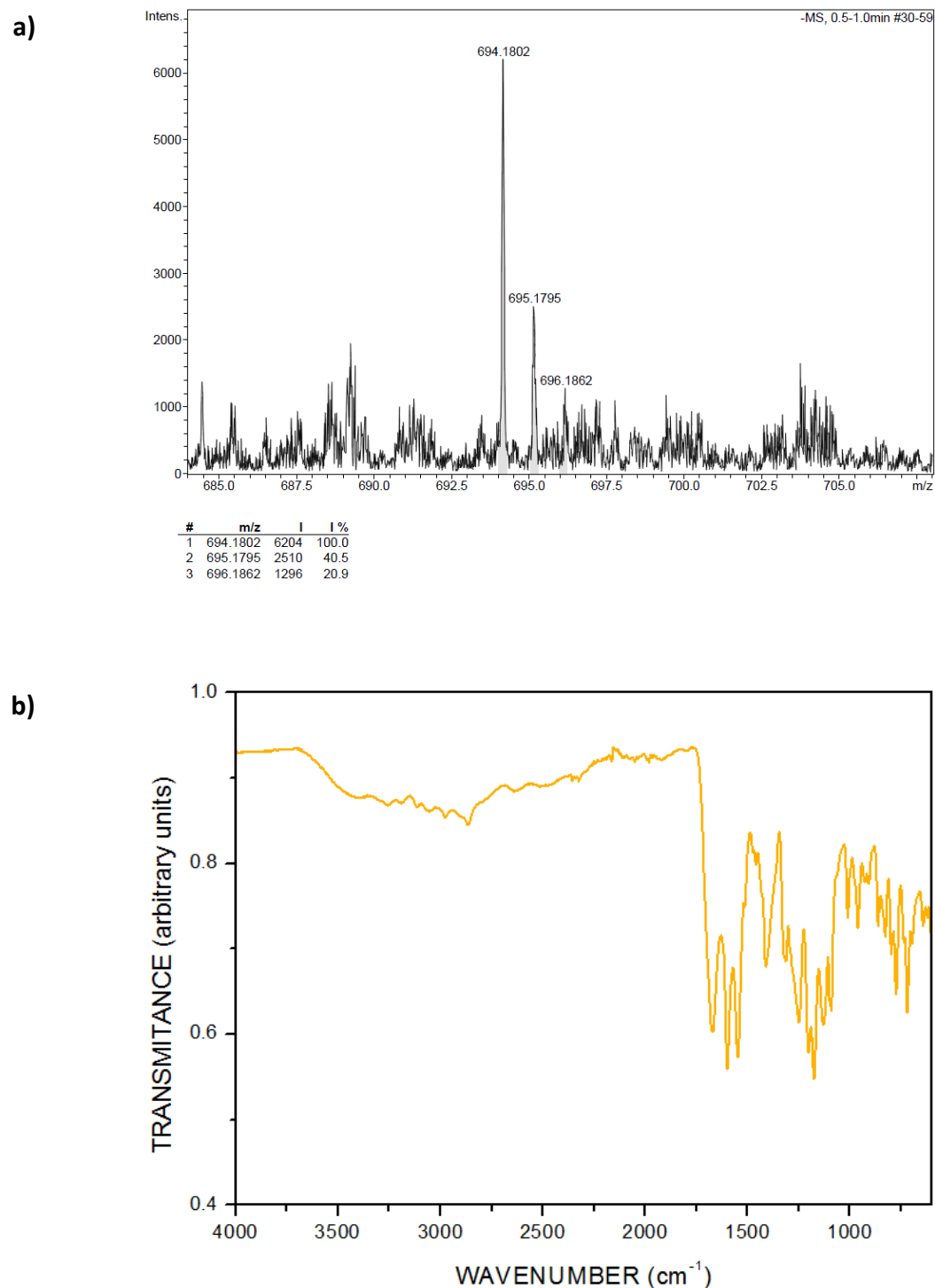


Figure S5. Characterization of **4**: (a) ESI-TOF/MS spectrum, and (b) FT-IR spectrum.

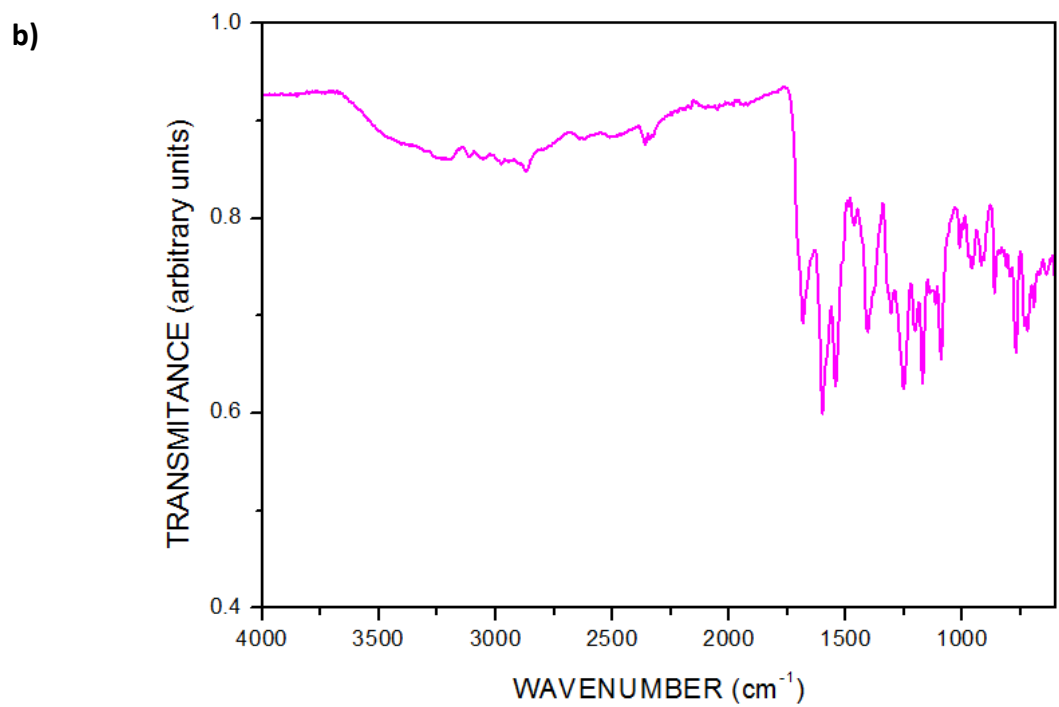
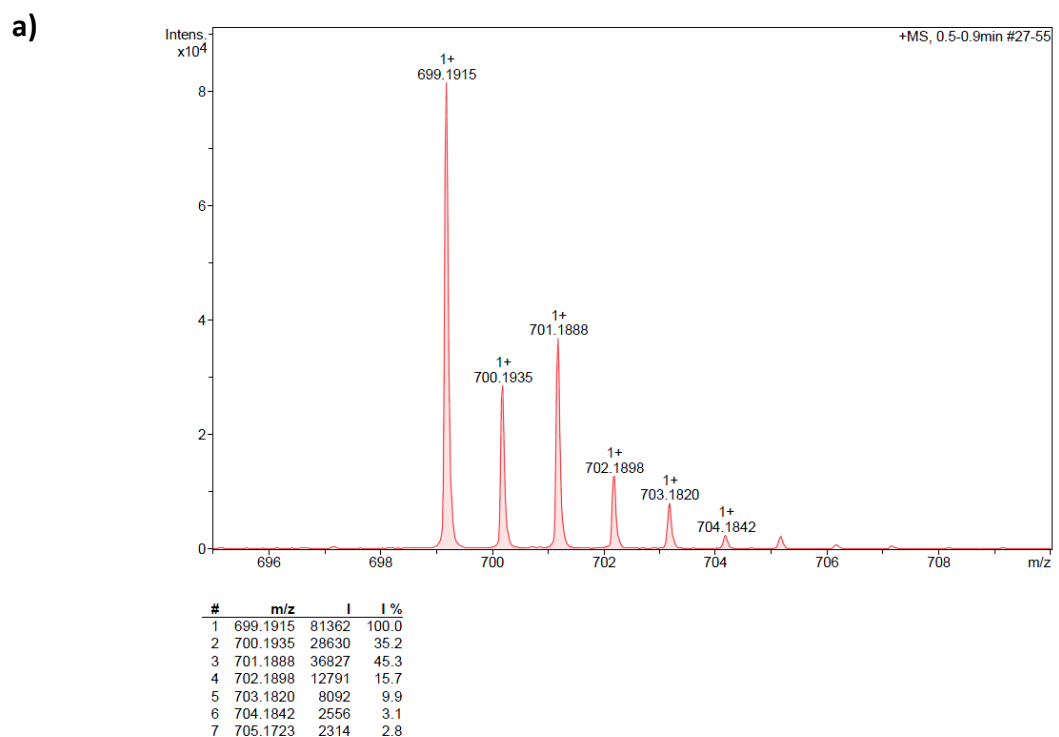
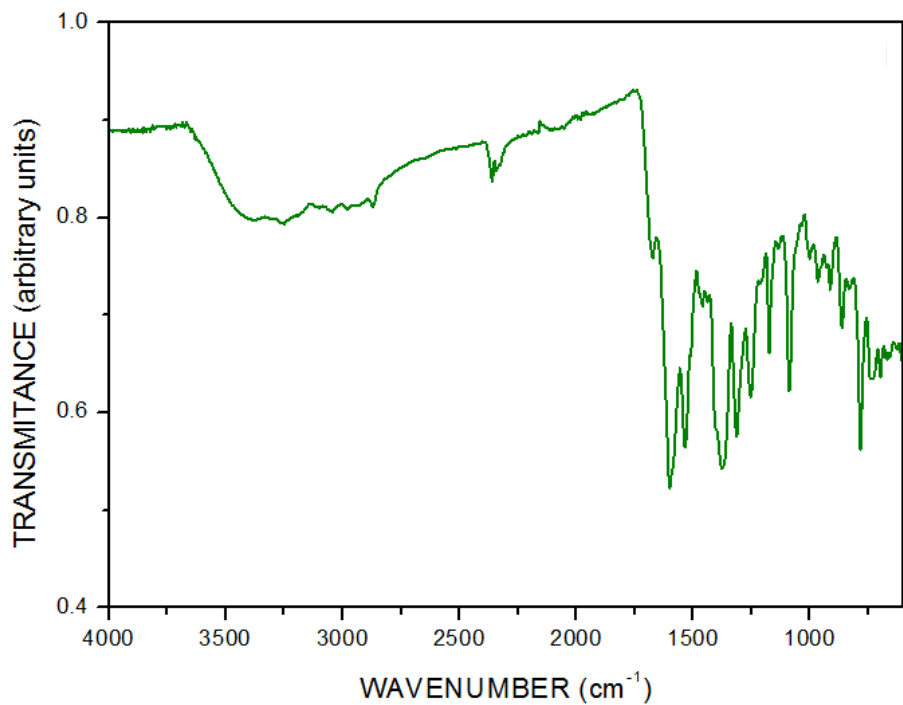


Figure S6. Characterization of **5**: (a) FT-IR spectrum, and (b) Powder X-Ray diffraction pattern of **5** (green), in comparison to the simulated pattern (black).

a)



b)

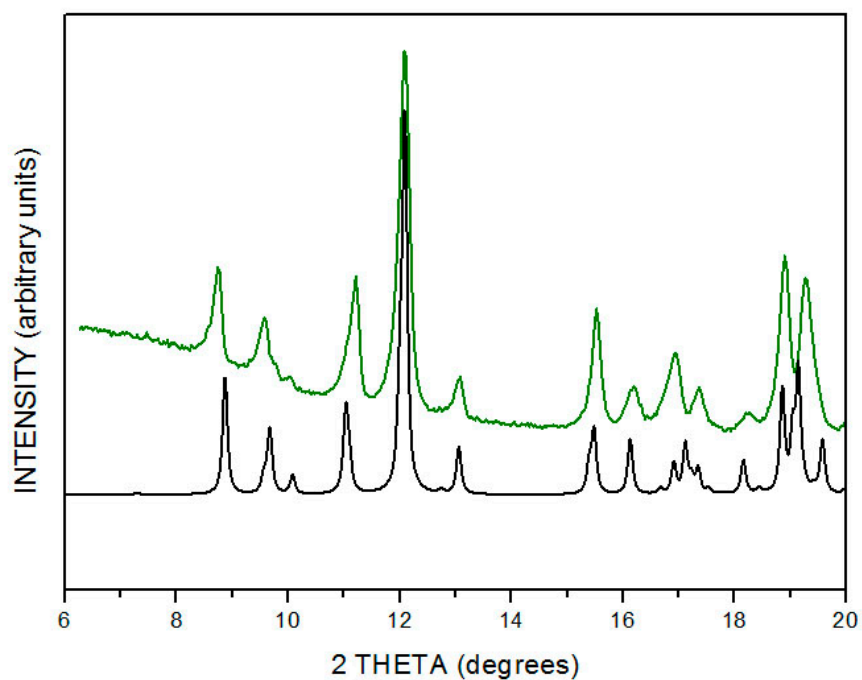


Figure S7. Characterization of **6**: (a) FT-IR spectrum, and (b) Powder X-Ray diffraction pattern of **6** (red), in comparison to the simulated pattern (black).

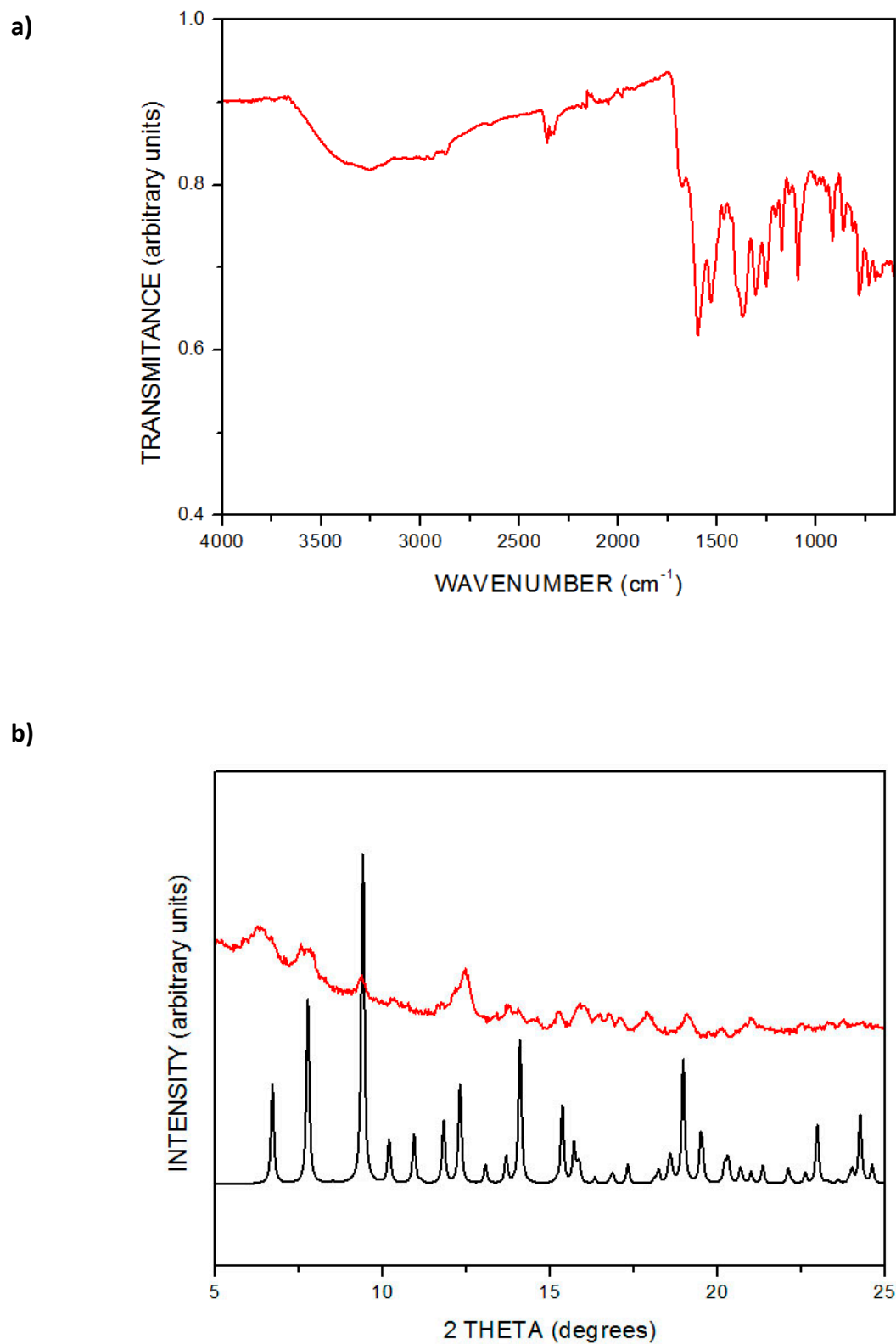


Figure S8. Characterization of **7**: (a) FT-IR spectrum, and (b) Powder X-Ray diffraction pattern of **7** (orange), in comparison to the simulated pattern (black).

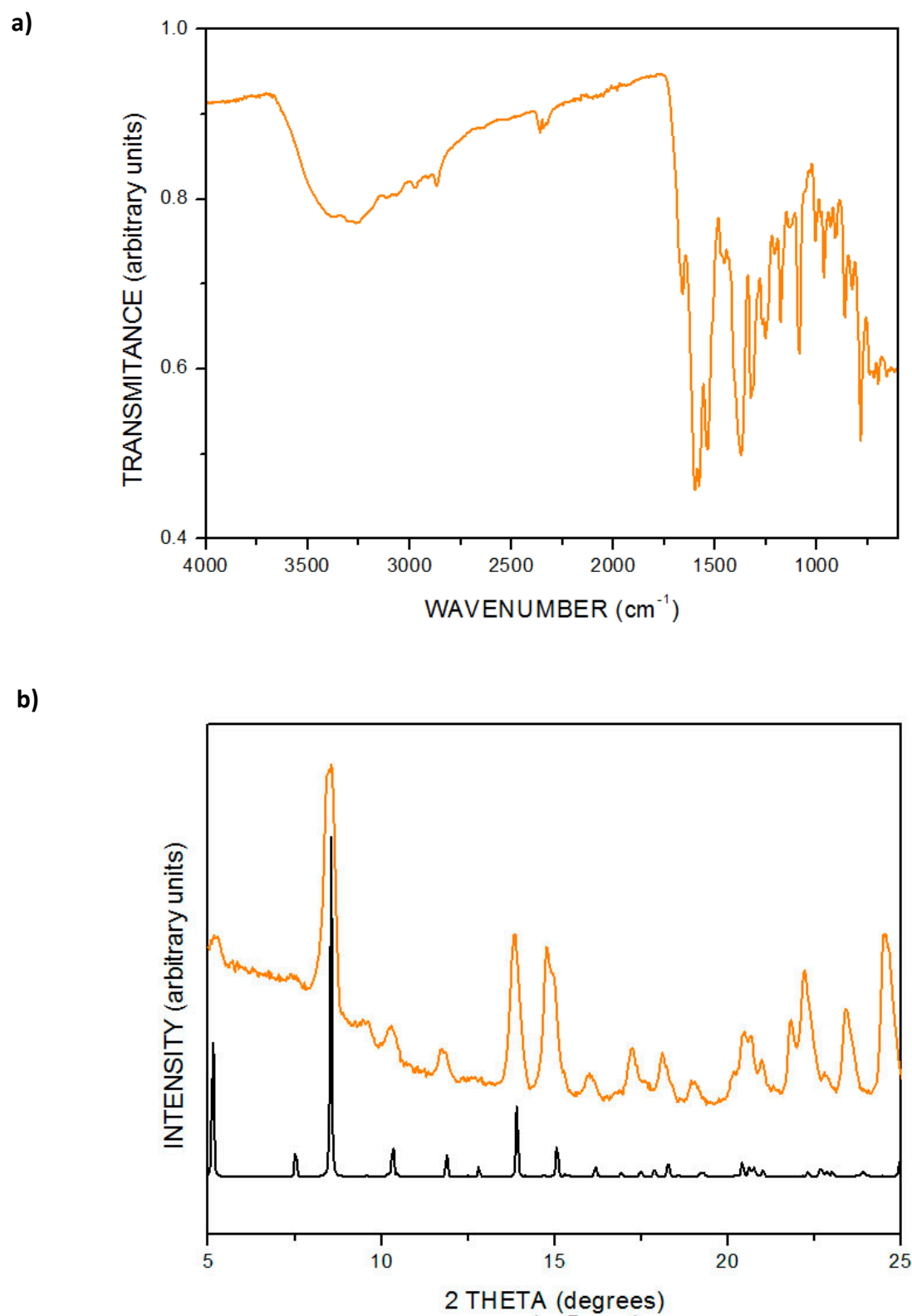
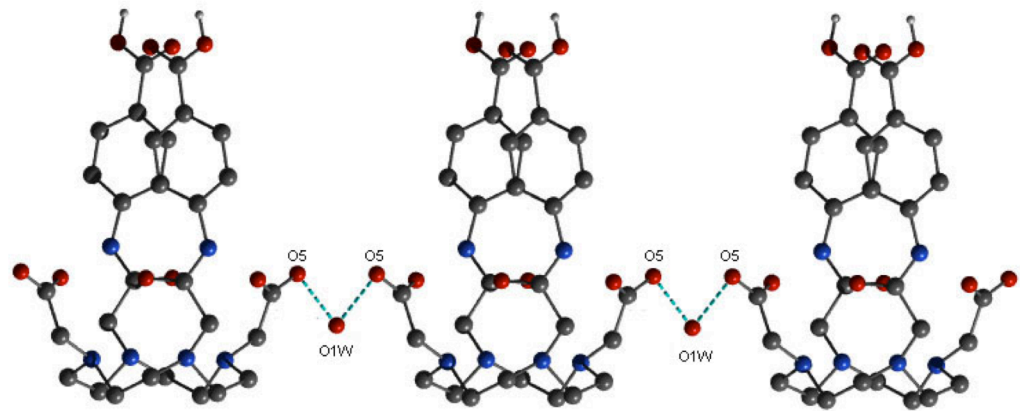
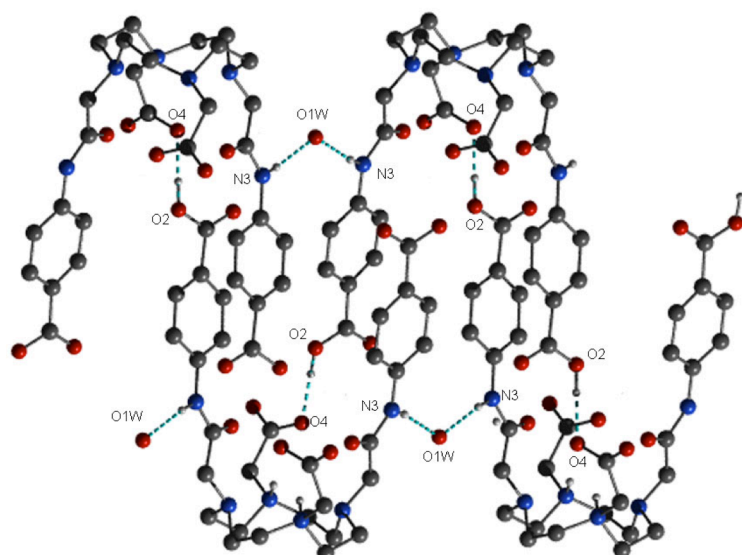


Figure S9. Views of the H-bonded packing of $\text{H}_4\text{L1}$. Hydrogen bonds are marked as sky blue dash lines. Hydrogen-bond geometry (\AA , $^\circ$) data is shown below.

a)



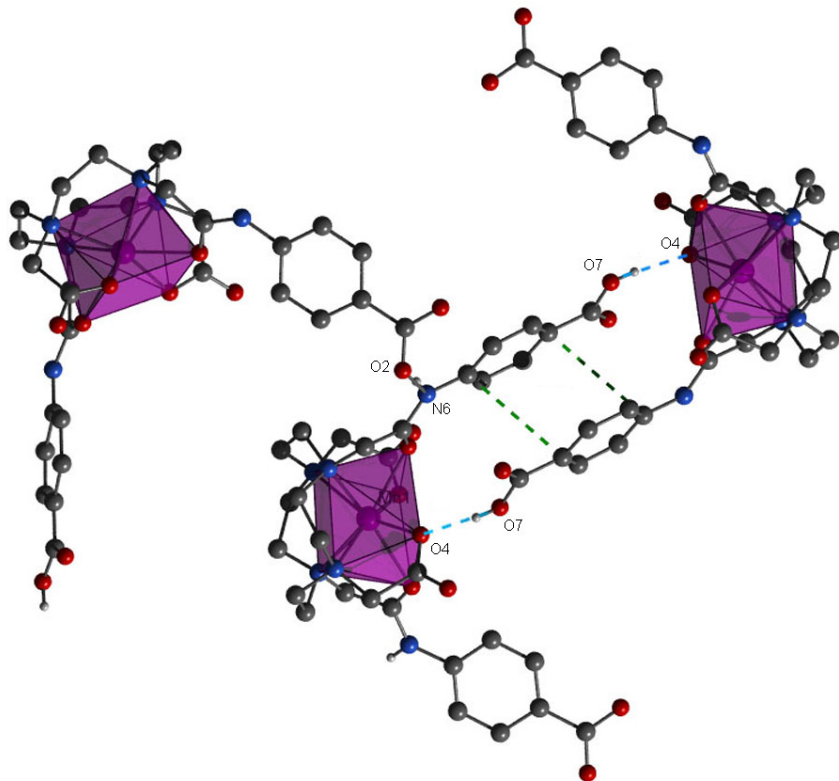
b)



$D-\text{H}\cdots A$	$D-\text{H}$	$\text{H}\cdots A$	$D\cdots A$	$D-\text{H}\cdots A$
$\text{N3}-\text{H}\cdots \text{O}1\text{W}^{\text{i}}$	0.86	2.16	3.004(8)	169
$\text{O}1\text{W}-\text{H}\cdots \text{O}5^{\text{ii}, \text{iii}}$	--	--	2.813(0)	--
$\text{O}2-\text{H}\cdots \text{O}4^{\text{iv}}$	0.92	1.67	2.592(0)	174

Symmetry codes: (i) $x, y, 1+z$; (ii) $1/2-x, 1/2-y, 1-z$; (iii) $-1/2+x, 1/2-y, -1/2+z$ (iv) $x, -y, 1/2+z$

Figure S10. View of the H-bonded packing of **3**. Hydrogen bonds are marked as sky blue dash lines, and $\pi\text{-}\pi$ stacking interactions are marked as green dash lines. Hydrogen-bond geometry (\AA , $^\circ$) data is shown below.

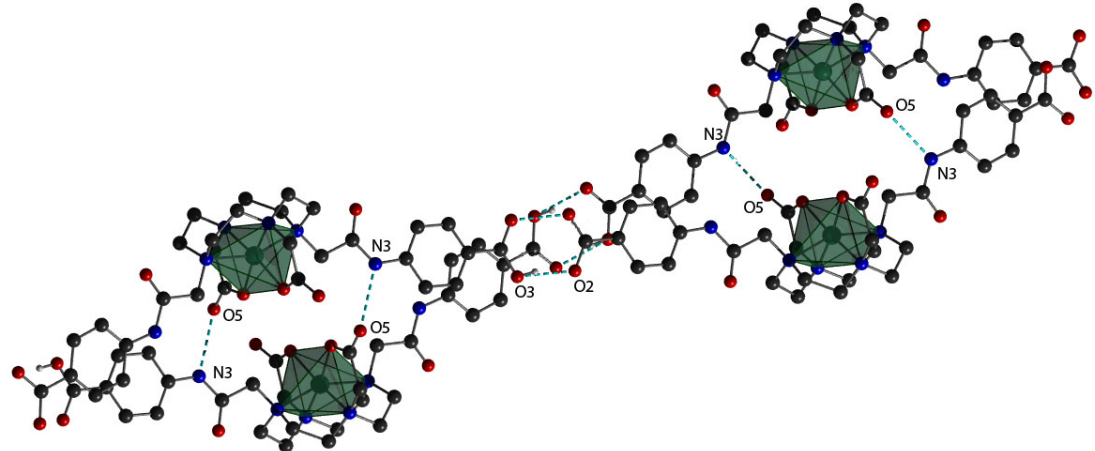


$D\text{--H}\cdots A$	$D\text{--H}$	$H\cdots A$	$D\cdots A$	$D\text{--H}\cdots A$
O7—H \cdots O4 ⁱ	0.82	1.71	2.510(8)	163

N6—H \cdots O2 ⁱⁱ	0.86	2.04	2.879(6)	164
--------------------------------	------	------	----------	-----

Symmetry codes: (i) 2-x, 1-y, 3-z; (ii) 2-x, -1/2+y, 5/2-z

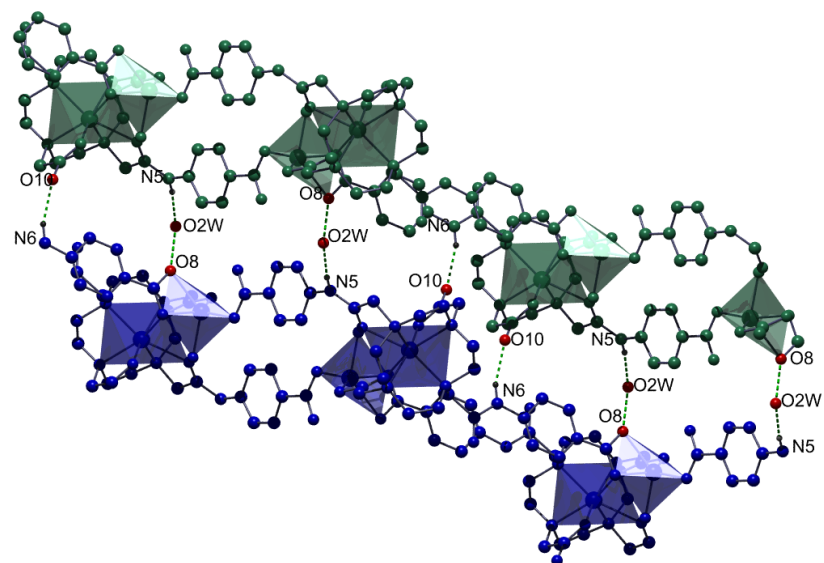
Figure S11. View of the H-bonded packing of **4**. Hydrogen bonds are marked as sky blue dash lines. Hydrogen-bond geometry (\AA , $^\circ$) data is shown below.



$D-\text{H}\cdots A$	$D-\text{H}$	$\text{H}\cdots A$	$D\cdots A$	$D-\text{H}\cdots A$
$O3-\text{H}\cdots O2^i$	0.82	1.82	2.628(7)	168
$N3-\text{H}\cdots O5^{\text{ii}}$	0.86	1.93	2.791(5)	176
$O1W-\text{H}\cdots O4^{\text{iii, iv}}$	--	--	3.022(4)	--

Symmetry codes: (i) $-x, -y, -2-z$; (ii) $1-x, -y, -z$; (iii) $x, -y, -1/2+z$; (iv) $1-x, -y, -z$

Figure S12. View of the H-bonded packing of the double-strand chains in **5**. Hydrogen bonds are marked as green dash lines. Hydrogen-bond geometry (\AA , $^\circ$) data is shown below.

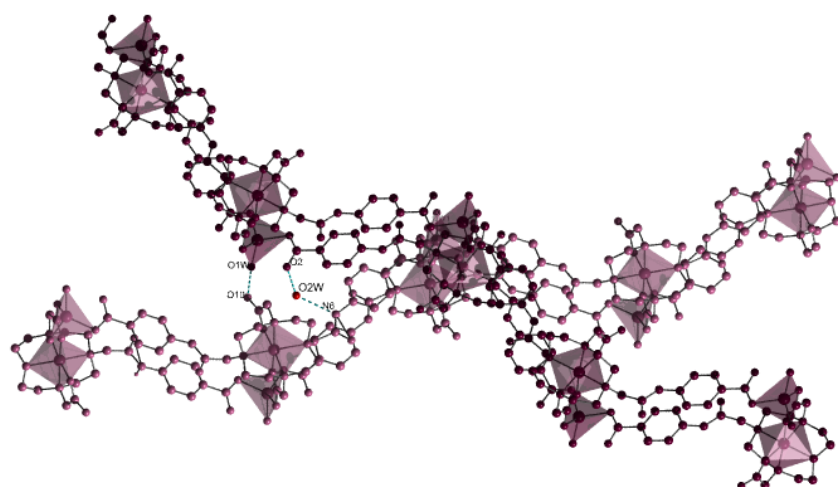


$D-\text{H}\cdots A$	$D-\text{H}$	$\text{H}\cdots A$	$D\cdots A$	$D-\text{H}\cdots A$
N6—H \cdots O10 ⁱ	0.86	2.03	2.852(6)	160
N5—H \cdots O2W	0.86	1.92	2.765(2)	169
O2W—H \cdots O8 ⁱ	--	--	2.850(3)	--

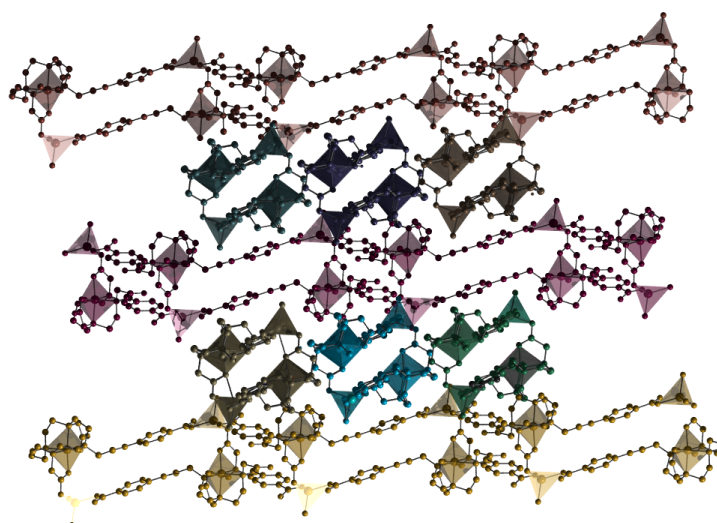
Symmetry codes: (i) 1-x, 1-y, -z

Figure S13. Views of a) the hydrogen bonds between double-strand chains in **6** and b) the packing of these double-strand chains along the [110] direction. Hydrogen bonds are marked as sky blue dash lines. Hydrogen-bond geometry (\AA , $^\circ$) data is shown below.

a)



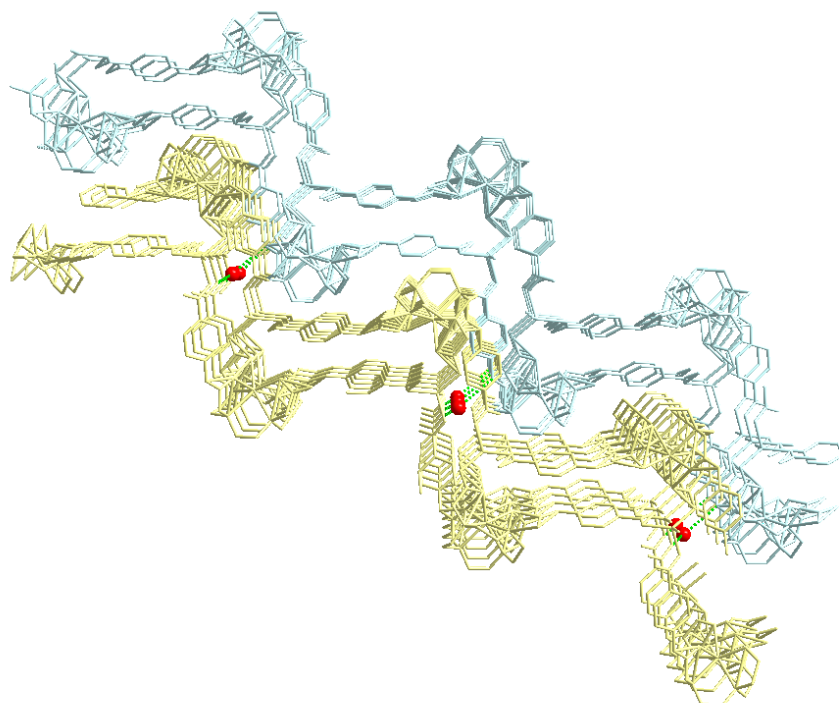
b)



$D-\text{H}\cdots A$	$D-\text{H}$	$\text{H}\cdots A$	$D\cdots A$	$D-\text{H}\cdots A$
N6—H \cdots O2W	0.86	2.02	2.874(5)	170
O2W—H \cdots O2 ⁱ	--	--	2.818(1)	--
O1W—H \cdots O10 ⁱⁱ	--	--	2.591(0)	--

Symmetry codes: (i) $1/2-x$, $-1/2+y$, $3/2-z$; (ii) $1/2+x$, $1/2-y$, $1/2+z$

Figure S14. View of the H-bonded packing of the layers of **7** via O4W water molecule along the *b* axis. Hydrogen bonds are marked as sky blue dash lines. Hydrogen-bond geometry (\AA , $^\circ$) data is shown below.



$D-\text{H}\cdots A$	$D-\text{H}$	$\text{H}\cdots A$	$D\cdots A$	$D-\text{H}\cdots A$
N5—H \cdots O4W ⁱ	0.86	2.13	2.941(7)	157
O4W—H \cdots O2	--	--	2.962(4)	--

Symmetry codes: (i) x, 2-y, -1/2+z

Figure S15. Powder X-Ray diffraction pattern resulting from the activated, amorphous 7' once it has been exposed to a water sorption/desorption cycle (blue), in comparison to the simulated pattern (black).

